1521-009X/50/11/1429–1433$35.00
Drug Metabolism and Disposition

dx.doi.org/10.1124/dmd.122.000919
Drug Metab Dispos 50:1429–1433, November 2022

Molecular and Functional Characterization of *N*-Acetyltransferases in Common Marmosets and Pigs

Yasuhiro Uno, Shotaro Uehara, Moe Ijiri, Hiroaki Kawaguchi, Atsushi Asano, Mitsuya Shiraishi, Kaito Banju, Norie Murayama, and Hiroshi Yamazaki

Joint Faculty of Veterinary Medicine, Kagoshima University, Kagoshima, Japan (Y.U., M.I., A.A., M.S.); Laboratory of Drug Metabolism and Pharmacokinetics, Showa Pharmaceutical University, Tokyo, Japan(S.U., K.B., N.M., H.Y.); and School of Veterinary Medicine, Kitasato University, Aomori, Japan (H.K.)

Received April 7, 2022; accepted June 8, 2022

ABSTRACT

Arylamine *N*-acetyltransferases (NATs) are drug-metabolizing enzymes that are essential for the metabolism of endogenous substrates and xenobiotics. The molecular characteristics of NATs have been extensively investigated in humans but remain to be investigated in common marmosets and pigs, animal species that are often used in drug metabolism studies. In this study, marmoset NAT1 and pig NAT1 cDNAs were isolated from liver samples and were characterized by molecular analyses and drug-metabolism assays. These *NAT* genes were intronless and formed gene clusters with one other *NAT* gene in the genome, just as human *NAT* genes do. Marmoset NAT1 and pig NAT1 amino acid sequences showed high sequence identities (94% and 85%, respectively) to human NAT1. Phylogenetic analysis indicated that marmoset NAT1 and pig NAT1 were more closely clustered with human NATs than with rat or mouse NATs. Marmoset NAT1 and pig NAT1 mRNAs were expressed in all the tissue types analyzed, with the expression levels being highest in the small intestine. Metabolic assays using recombinant proteins found that marmoset NAT1 and pig NAT1 metabolized human NAT substrates *p*-aminobenzoic acid, 2-aminofluorene, sulfamethazine, and isoniazid. Marmoset NAT1 and pig NAT1 substantially acetylated *p*-aminobenzoic acid and 2-aminofluorene relevant human NAT1, but their activities were lower toward sulfamethazine and isoniazid than those of the relevant human NAT2. Therefore, marmoset and pig NATs are functional enzymes with molecular similarities to human NAT1, but their substrate specificities, while similar to human NAT1, differ somewhat from human NAT2.

SIGNIFICANCE STATEMENT

Marmoset *N*-acetyltransferase NAT1 and pig NAT1 were identified and showed high sequence identities to human NAT1. These NAT mRNAs were expressed in various tissues. Marmoset and pig NAT1s acetylated typical human NAT substrates, although their substrate specificities differed somewhat from human NAT2. Marmoset NAT1 and pig NAT1 have similarities with human NAT1 in terms of molecular and enzymatic characteristics.

Introduction

Species differences in the clearance of drug candidates represent an important issue during drug development. Consequently, it is essential to carefully select the animal species used for drug metabolism studies. To predict the human pharmacokinetic profiles of drug candidates, nonhuman primates (e.g., cynomolgus macaques), pigs, and dogs are often used in addition to rats. Pigs are used as animal models for various biomedical studies because of their similarities to humans in terms of size, physiology, and susceptibility to disease. Recent studies have shown the functional similarities of cytochrome P450 enzymes in humans and in the New World monkey *Callithrix jacchus*, or common marmoset, indicating the potential usefulness of this nonhuman primate species for preclinical testing (Uno et al., 2016).

Arylamine *N*-acetyltransferases (NATs) are enzymes that acetylate xenobiotics, including environmental carcinogens and drugs (Sim et al., 2008; Zhou et al., 2013; Sim et al., 2014). NAT1 and NAT2 have been identified in humans; NAT1 substrates include *p*-aminosalicylate, whereas NAT2 substrates include hydralazine, procainamide, and isoniazid (Sim et al., 2008; Sim et al., 2014). In contrast, 5-aminosalicylic acid, 4-bromoaniline, and 4-iodoaniline are acetylated by both human NATs (Sim et al., 2008; Sim et al., 2014). Therefore, NAT1 and NAT2 show different, but overlapping, substrate specificities. In humans, expression of NAT2 mRNA is mainly detected in the liver and intestine, whereas expression of NAT1 mRNA is evident in various tissues, including the liver and intestine (Jennne, 1965; Hickman et al., 1998; Boukouvala and Fakis, 2005).

In humans, genetic variants affect the enzyme functionality of NAT1 and NAT2 (Walraven et al., 2008a; Walraven et al., 2008b; Hein, 2009). For example, R64W reduces the enzymatic activity of NAT1 and NAT2, and D122N inactivates NAT2 (Walraven et al., 2008b; Hein, 2009). Similarly, in cynomolgus macaques, D122N reduces NAT1 activity, and T98A reduces NAT2 activity (Uno et al., 2020). NATs represent an early example of pharmacogenetic variation and established the basis of understanding variability in drug metabolism among different populations (Sim et al., 2014). Therefore, genetic variants are also important for understanding the properties of NAT enzymes.

In marmosets and pigs, drug-metabolizing enzymes such as cytochromes P450 have been identified and analyzed; however, NATs have

This work was supported partly by the Japan Society for the Promotion of Science Grant-in-Aid for Scientific Research [Grant 20K06434].

The authors have no competing interests to declare.

dx.doi.org/10.1124/dmd.122.000919.

ABBREVIATIONS: NAT, *N*-acetyltransferase; PCR, polymerase chain reaction; RT, reverse transcription.

not yet been characterized in these species. In this study, therefore, we isolated marmoset NAT1 and pig NAT1 cDNAs from liver samples and characterized the new forms by sequence and phylogenetic analyses, tissue expression analyses, and enzymatic assays.

Materials and Methods

Materials. Oligonucleotides were synthesized by Integrated DNA Technologies (Coralville, IA). *p*-Aminobenzoic acid, 2-aminofluorene, sulfamethazine, isoniazid, and acetyl-coenzyme A were obtained from Fujifilm Wako Pure Chemicals (Osaka, Japan), *N*-acetyl *p*-aminobenzoic acid and 2-acetylaminofluorene were from Sigma-Aldrich (St. Louis, MO), *N*-acetyl sulfamethazine from Santa Cruz Biotechnology (Dallas, TX), and *N*-acetyl isoniazid from Toronto Research Chemicals (North York, ON, Canada). All other reagents were purchased from Sigma-Aldrich or Fijifilm Wako Pure Chemicals, unless otherwise specified.

Tissues and Preparation of RNA and Cytosol. Tissue samples (adrenal gland, brain, heart, ileum, jejunum, kidney, liver, lung, ovary, and uterus) were collected from a pig (Microminipig, female, 10 years of age, weight 13 kg) at Kagoshima University. From these samples, total RNA was extracted using an RNeasy Mini Kit (Qiagen, Valencia, CA) according to the manufacturer's protocols and used for cDNA cloning and analysis of tissue expression patterns. Tissue RNA samples (brain, lung, liver, kidney, and small intestine) of marmosets (three males and three females) were obtained as previously described (Uehara et al., 2016b; Uehara et al., 2020). Liver cytosol samples were prepared as described previously (Uehara et al., 2017; Uehara et al., 2020). This study was reviewed and approved by the Institutional Animal Care and Use Committee at Kagoshima University.

Molecular Cloning. To isolate marmoset NAT1 and pig NAT1 cDNAs, reverse transcription (RT)-polymerase chain reaction (PCR) was performed using liver total RNA in a similar manner to that described in our previous study (Uno et al., 2006). Briefly, first-strand cDNA synthesis was carried out in a reaction mixture containing 1 μg of total RNA, oligo (dT), and ReverTra Ace (TOYOBO, Osaka, Japan) at 42°C for 1 hour according to the manufacturer's protocols. PCR reactions were performed using the RT product as the template with Q5 Hot Start High-Fidelity DNA Polymerase (New England BioLabs, Ipswich, MA) and a T100 thermal cycler (Bio-Rad Laboratories, Hercules, CA) according to the manufacturers' protocols. PCR conditions were an initial denaturation at 98°C for 30 seconds; followed by 35 cycles at 98°C for 10 seconds, 60°C for 20 seconds, and 72°C for 20 seconds; followed by a final extension at 72°C for 2 minutes (annealing was done at 65°C for marmoset NAT1). The primers used were cjNAT1 (5rt1) 5′-GGGATCATGGACATTGAAGCATATC-3′ and cjNAT1 (3rt1) 5′-CAGTTGATAACTGGTGAGCTAGGTAATAAATACAC-3′ for marmoset NAT1, and pNATv2 (5rt1) 5′-CGGGAATCATGAACATTGAAGCATAC-3′ and pNATv2 (3rt1) 5′-ATGTTACAGCATCAGATAGCATATTGATACCATTT-3′ for pig NAT1. The amplified products were cloned into pMiniT2.0 vectors using a PCR Cloning Kit (New England BioLabs) according to the manufacturer's protocol. The inserts were sequenced using an ABI PRISM BigDye Terminator v3.0 Ready Reaction Cycle Sequencing Kit (Applied Biosystems, Foster City, CA) with an ABI PRISM 3500xl Genetic Analyzer (Applied Biosystems).

Sequence Analysis. Sequence data were analyzed using the Genetyx system (Software Development, Tokyo, Japan), including the ClustalW program, which was used for multiple alignment of amino acid sequences. A phylogenetic tree was created by the neighbor-joining method. BLAST (National Center for Biotechnology Information) was used for the homology search. BLAT (UCSC Genome Bioinformatics) was used for analysis of the human, marmoset, and pig genome data. Amino acid and cDNA sequences used for the analyses were from GenBank or the present study.

Measurement of mRNA Expression. Expression levels of pig NAT1 mRNA were measured in adrenal gland, brain, heart, ileum, jejunum, kidney, liver, lung, ovary, and uterus using real-time RT-PCR with gene-specific primers, as reported previously (Uno et al., 2006). Similarly, expression levels of marmoset NAT1 mRNA were measured in brain, kidney, liver, lung, and small intestine. Briefly, RT reactions were carried out using a ReverTra Ace qPCR RT kit (TOYOBO) or a High-Capacity cDNA Reverse Transcription Kit (Applied Biosystems) according to the manufacturer's protocols, and one-twentieth of the reaction mixture was subsequently used for PCR. The PCR amplification was carried out in a total volume of 20 μl using a THUNDERBIRD SYBR qPCR Mix Kit (TOYOBO) with a StepOnePlus Real-Time PCR System or a 7500 Fast Real-Time PCR system (Applied Biosystems), following the manufacturers' protocols. The following primers were used at final concentrations of 300 nM: cjNAT1 (5qrt1) 5′-GAAAGCAGCAAATACCGAAAAATC-3′ and cjNAT1 (3qrt1) 5′-TGCTAGTAAATACAGATGCTGGAGATG-3′ for marmoset NAT1, and pNATv2 (5qrt1) 5′-CAACACTTTTGCCGACAAATACA-3′ and pNATv2 (3qrt1) 5′-CACATCTGGTAAGAACGTCCAA-3′ for pig NAT1. The relative expression levels were determined, based on three independent amplifications, by normalizing the raw data to the 18S ribosomal RNA level, which was measured using TaqMan Gene Expression Assays (Assay ID: Hs99999901_s1, Applied Biosystems) with THUNDERBIRD Probe qPCR Mix (TOYOBO).

Heterologous Protein Expression in Escherichia coli. Expression plasmids were prepared and used to express marmoset NAT1 and pig NAT1 proteins as described previously (Uno et al., 2018). PCR was performed using Q5 Hot Start High-Fidelity DNA Polymerase (New England BioLabs), as described earlier, with the NAT cDNA as a template to generate expression plasmids. The primers used were cjNAT1 (5exp1) 5′-ATGGACATTGAAGCATATCTTG-3′ and cjNAT1 (3exp1) 5′-CCGCTCGAGTTGATAACTGGTGAGCTAGGTAAT-3′ for marmoset NAT1, and pNATv2 (5exp1) 5′-ATGAACATTGAAGCATACTT CAAAAGAATTGG-3′ and pNATv2 (3exp1) 5′-CCGCTCGAGCAGCATCA GATAGCATATTGATACCAT-3′ for pig NAT1. The reverse primers contained XhoI restriction enzyme site sequences (underlined) to facilitate subcloning of the PCR products into vectors. After restriction-enzyme digestion, the amplified DNAs were subcloned into a pET30a vector (Novagen, Madison, WI), which provides a 6×His-tag at the *N*-terminus. The prepared plasmids were used for protein expression, which was performed in *Escherichia coli*, followed by the preparation of cytosolic fractions as described previously (Uno et al., 2018).

Enzyme Assays. The acetyl-CoA–dependent acetylations at substrate concentrations of 30 μM and 300 μM of *p*-aminobenzoic acid, 2-aminofluorene, sulfamethazine, and isoniazid (Uno et al., 2020) were determined using a reversed-phase liquid chromatography as described previously (Uno et al., 2018). Typical reaction mixtures of 200 μL containing NAT protein (40 pmol equivalents/mL) or liver cytosolic fractions from marmosets, pigs, and humans (0.40 mg/mL), each substrate, and 1 mM dithiothreitol in 20 mM sodium phosphate buffer (pH 8.0) were initiated by the addition of acetyl-CoA (1.0 mM). After incubation at 37°C for 10 minutes (30 minutes for isoniazid acetylation by recombinant NAT proteins), the reaction was terminated by adding 25 μL of ice-cold 1.0 M acetic acid. The rates of acetylated metabolite formation were determined using an analytical reverse-phase C_{18} column (4.6 × 150 mm) eluted with a mixture of 20% (v/v) methanol in 10 mM acetate buffer (pH 4.0) at a flow rate of 1.0 mL/min with UV monitoring at 280 nm (Uno et al., 2018). The acetylated metabolites had longer retention times than the substrates under the present conditions. The catalytic activities of liver cytosolic fractions/recombinant NAT proteins are expressed as the nanomoles of substrates acetylated per minute per milligram of protein/nmol NAT. Data are mean and SD values from triplicate determinations unless specified.

Statistical analysis. Two-way analysis of variance with Bonferroni's post-hoc test was carried out using Prism (GraphPad Software, La Jolla, CA) to compare the levels among the groups.

Results

Identification and Analysis of Marmoset and Pig NAT cDNAs. Analysis of marmoset and pig genome data found gene sequences highly homologous to human *NAT* genes; these sequences were designated *NAT1* in both species. The marmoset and pig *NAT1*s formed gene clusters in the genome with one other *NAT*, similar to their human orthologs, but with some differences (Fig. 1). The direction of pig *NAT1* was opposite to that of human *NAT2*, and marmoset *NATP* contained a partial sequence (Fig. 1). Based on these *NAT* sequences, gene-specific primers were designed, and marmoset NAT1 and pig NAT1 cDNAs were successfully isolated from liver by RT-PCR. However, pig NAT2 cDNA could not be isolated despite several trials using different primers. The coding regions of marmoset *NAT1* and pig *NAT1* were intronless, just as they are in human *NAT*s. Marmoset NAT1 and pig NAT1 amino acid sequences of 290 residues were highly identical (94% and 85%) to human NAT1 but were less identical to human

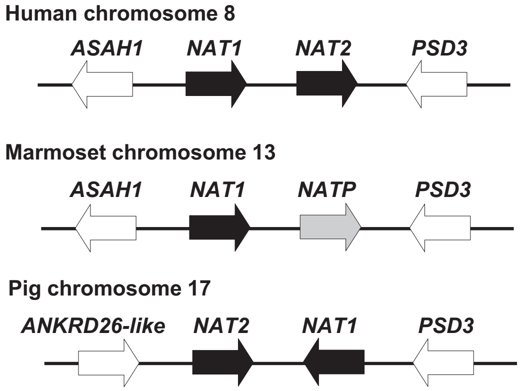

Fig. 1. Arrangement of *NAT* genes in the marmoset and pig genomes. The marmoset, pig, and human genomes were analyzed using BLAT. Two *NAT* genes formed a gene cluster in the marmoset and pig genomes, similar to that in the human genome, but one of the marmoset *NAT* genes was pseudogenized, and pig *NAT1* ran in the opposite direction to human and marmoset *NAT1*. The indicated sizes of the genes and the distances between them are not proportional to actual measurements.

TABLE 1

Sequence identities of marmoset and pig NATs compared with human NATs. *Marmoset and pig NAT amino acid and cDNA sequences (coding regions) were compared with human sequences using BLAST.*

		Sequence Identity	
	Human	Amino acids	cDNA
		%	
Marmoset NAT1	NAT1	**94**	**95**
	NAT2	80	87
Pig NAT1	NAT1	**85**	**83**
	NAT2	77	81

NAT2 (80% and 77%, Table 1). The primary sequence structures of marmoset and pig NAT1 were characteristic of NAT proteins, i.e., I/VPFENLxx, RGGfCdrxxxf, DaGdjj (Payton et al., 2001), and a catalytic triad (Cys68, His107, Arg122) were conserved in marmoset, pig, and human NATs (Fig. 2). Phylogenetic analysis revealed that marmoset NAT1 and pig NAT1 were more closely clustered with human NATs than with rat or mouse NATs (Fig. 3). Marmoset NAT1 was closely related to human NAT1, whereas pig NAT1 did not show a one-to-one relationship with human NATs. The marmoset and pig NAT1 cDNAs identified in the current study have been deposited to GenBank under accession numbers ON191586 and ON191585, respectively.

Tissue Expression Patterns of Marmoset and Pig NAT mRNAs. To measure the expression levels of marmoset NAT1 and pig NAT1 mRNAs, real-time RT-PCR was performed in samples of pig adrenal gland, brain, heart, ileum, jejunum, kidney, liver, lung, ovary, and uterus and in marmoset brain, lung, liver, kidney, and small intestine. Pig NAT1 mRNA was expressed in all the tissues tested, including liver and kidney, but with most abundant expression in ileum and jejunum (Fig. 4). Marmoset NAT1 mRNA was also expressed in all the tissues analyzed, but the expression level was highest in the small intestine, followed by kidney, lung, and liver (Fig. 4). In the small intestine, marmoset NAT1 mRNA was more abundant (~3.2-fold) in males than females significantly ($p < 0.001$); however, there were no major sex differences (>twofold) in other tissue types.

Drug-metabolizing Activities of NAT Proteins. Liver cytosolic fractions from marmosets and pigs showed NAT activities toward typical human NAT substrates (*p*-aminobenzoic acid, 2-aminofluorene, sulfamethazine, and isoniazid) similar to those from humans (Fig. 5A). Among these substrates, marmosets showed lower activities toward sulfamethazine. In consideration of an illustrated pattern of catalytic activities, marmoset and pig NAT proteins heterologously expressed in *E. coli* showed activities toward all these human NAT substrates, similar to those previously reported for human NAT1 protein (Uno et al., 2018) (Fig. 5, B and C). Taken together, these results indicated that marmoset and pig NATs are functional enzymes similar to human NAT1 with distinct but overlapping substrate specificities.

Discussion

In this study, marmoset and pig NAT cDNAs were identified and characterized by sequence and phylogenetic analyses, tissue expression pattern analysis, genome structure, and enzymatic assays. Marmoset NAT1 and pig NAT1 sequences were highly identical to human NAT1 (Table 1), contained characteristic motifs of NAT proteins (Fig. 2), and were clustered with human NATs more closely than with rodent NATs in a phylogenetic tree (Fig. 3). Moreover, clusters of two *NAT* genes

```
hNAT1    1:MDIEAYLERIGYKKSRNKLDLETLTDILQHQIRAVPFENLNIHCGDAMDLGLEAIFDQVVRRNRGGWCLQVNHLLYWALTTIGFETTMLGGYVYSTPAKK 100
hNAT2    1:MDIEAYFERIGYKNSRNKLDLETLTDILEHQIRAVPFENLNMHCGQAMELGLEAIFDHIVRRNRGGWCLQVNQLLYWALTTIGFQTTMLGGYFYIPPVNK 100
cjNAT1   1:MDIEAYLERIGYKKSRNKLDLETLTDILQHQIRAVPFENLNIHCGEAMDLDLGAIFDQIVRRNRGGWCLQVNHLLYWALTTIGFETTILGGYVYSTPAKK 100
pNAT1    1:MNIEAYFKRIGYKNWKNKLDLETLTDILQHQIRAIPFENLNIHCGEAMELDLEAIFDQIVRRNRGGWCLQVNHLLYWALTTIGFETTILGGYVYNTFADK 100
             *.**** .***** ..************.*****.******.*** ** * *.****..*************.***********.** ****.* ... *

hNAT1  101:YSTGMIHLLLQVTIDGRNYIVDAGFGRSYQMWQPLELISGKDQPQVPCVFRLTEENGFWYLDQIRREQYIPNEEFLHSDLLEDSKYRKIYSFTLKPRTIE 200
hNAT2  101:YSTGMVHLLLQVTIDGRNYIVDAGSGSSSQMWQPLELISGKDQPQVPCIFCLTEERGIWYLDQIRREQYITNKEFLNSHLLPKKKHQKIYLFTLEPRTIE 200
cjNAT1 101:YSTGMIHLLLQVTIDGKNYIVDAGFGRSYQIWQPLELISGKDQPQVPCIFRLTEENGFWYLDQIRRDQYIPNEEFLNSDLIESSKYRKIYSFTLEPRTIE 200
pNAT1  101:YSNAMIHLLLKVAIDGREYIVDAGFGRSYQMWQPLELISGKDQPQVPCIFRLREEEGIWYLDQIRREQYIANEEFLNSDLLEMNNYRKIYSFTLEPRTIE 200
             **..*.****.*.***..******.*.*.*.****************.*.*.** * ********.*** *.***.*.*..  ...***.***.*****

hNAT1  201:DFESMNTYLQTSPSSVFTSKSFCSLQTPDGVHCLVGFTLTHRRFNYKDNTDLIEFKTLSEEEIEKVLKNIFNISLQRKLVPKHGDRFFTI           290
hNAT2  201:DFESMNTYLQTSPTSSFITTSFCSLQTPEGVYCLVGFILTYRKFNYKDNTDLVEFKTLTEEEVEEVLRNIFKISLGRNLVPKPGDGSLTI           290
cjNAT1 201:DFESMNTYLQTSPASVFTSKSFCSLQTPEGVHCLVGFTLTYRRFNYKDNTDLIEFKTLNEEEIEKALKNIFNISLERKLVPKHGDRFFTI           290
pNAT1  201:DFESVNIYLQESPASVFTSKSFCSLQTPEGVHCLVGFTLTYRRFNYKDNMDLVEFKTLKVEEIEEELKSIFNISLEKKLVPKHGDRFFTI           290
             ****.*.***.** *.*...********.**.*****.**.*.******.** ***** .**.* *..**.*** ..****.**...**
```

Fig. 2. Multiple alignment of marmoset, pig, and human NAT sequences. Marmoset NAT1 and pig NAT1 were aligned with human NAT1 and NAT2. The sequence motifs characteristic of NAT proteins (I/VPFENLxx, RGGfCdrxxxf, and DaGdjj) and catalytic triad residues, respectively, are indicated by the solid lines and arrows above the sequences. Identical and conserved residues, respectively, are indicated with asterisks and dots under the sequences.

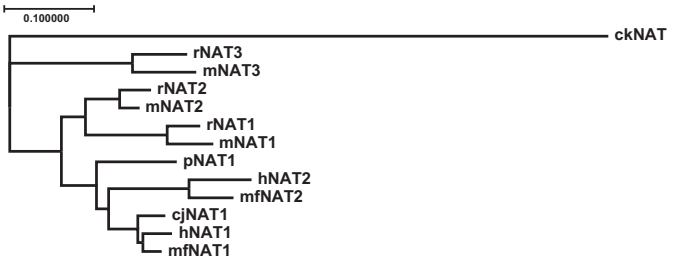

Fig. 3. Phylogenetic tree of NAT sequences. The phylogenetic tree was created by the neighbor-joining method using NAT amino acid sequences from humans (h), cynomolgus macaques (mf), marmosets (cj), pigs (p), rats (r), and mice (m). Chicken NAT (ckNAT) was used as the outgroup. The scale bar indicates 0.1 amino acid substitutions per site for distance measurement.

were located in the marmoset and pig genomes, similar to the arrangement in the human genome; however, one marmoset gene was pseudogenized, and one pig gene was located in the opposite direction (Fig. 1). Therefore, marmoset and pig *NAT*s have molecular characteristics similar to those of human *NAT*s.

Marmoset and pig NAT mRNAs were expressed in various tissues but were most abundantly expressed in the small intestine (Fig. 4). In humans, NAT1 mRNA is expressed in various tissues, whereas NAT2 mRNA is preferentially expressed in the liver and intestine (Boukouvala and Fakis, 2005; Husain et al., 2007b). These distinct expression patterns in humans might be accounted for by differences in upstream regulatory elements, including an active Sp1 box that is located in *NAT1* (Husain et al., 2007a) but not in *NAT2* (Husain et al., 2007b). The expression patterns of marmoset NAT1 and pig NAT1 mRNAs might reflect those of human NAT1. It would be of great interest to investigate the regulatory mechanism(s) of marmoset *NAT1* and pig *NAT1*.

Marmoset and pig NAT proteins acetylated typical human NAT substrates, including *p*-aminobenzoic acid, 2-aminofluorene, sulfamethazine, and isoniazid (Fig. 5A), and thus were functional enzymes. Marmoset and pig NAT1 efficiently acetylated *p*-aminobenzoic acid, a selective substrate of human NAT1, but their acetylation activities were not as efficient with respect to sulfamethazine and isoniazid (Fig. 5B), which are selective substrates of human NAT2 (Fig. 5C), possibly because of their high sequence identities to human NAT1 (Table 1) (Uno et al., 2018). In addition to 2-aminofluorene like a multi-NAT probe, in cynomolgus macaques, *p*-aminobenzoic acid and isoniazid are more efficiently acetylated by NAT1 and NAT2, respectively, similar to humans, but

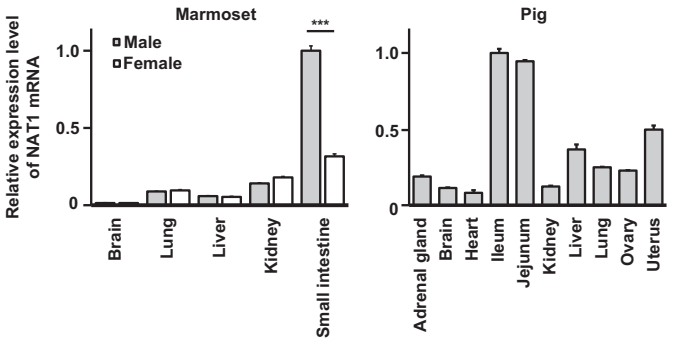

Fig. 4. Tissue expression patterns of marmoset and pig NAT mRNAs. Marmoset NAT1 and pig NAT1 mRNAs were measured by real-time RT-PCR in various tissues. Marmoset NAT1 mRNA levels were compared between males and females. The NAT mRNA levels were normalized to 18S rRNA levels and are shown as the average ± S.D. from three independent amplifications. The most abundant expression level was arbitrarily adjusted to 1, with which all other expression levels were compared. ***$P < 0.001$.

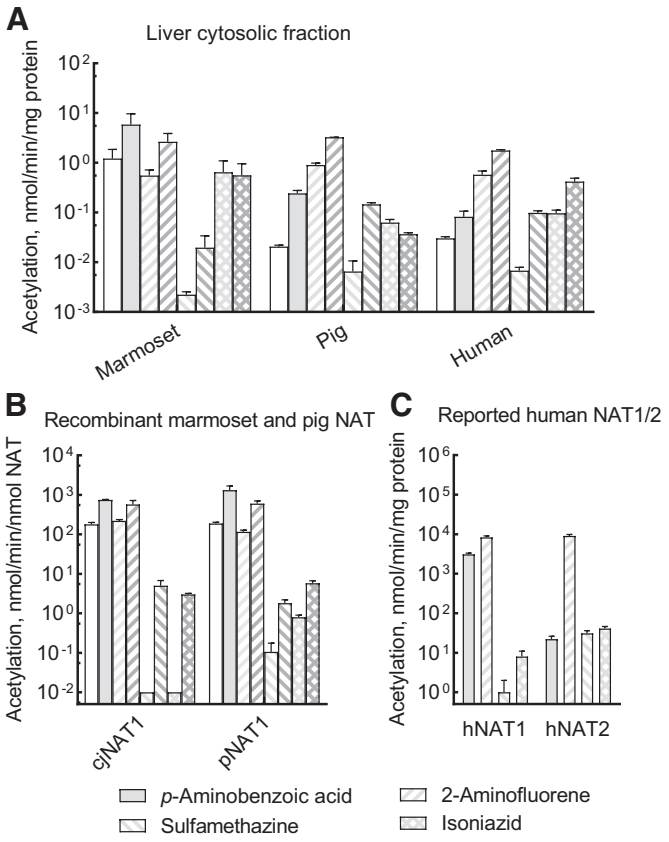

Fig. 5. Catalytic activities of marmoset and pig NATs. Acetylation activities were measured using human NAT substrates (*p*-aminobenzoic acid, open and closed bars; 2-aminofluorene, light and dark hatched bars; sulfamethazine, light and dark reversed hatched bars; and isoniazid, light and dark crossed bars) in marmoset, pig, and human liver cytosolic fractions (A) and marmoset (cj) and pig (p) NAT proteins (B) at substrate concentrations of 30 μM (light gray bars) and 300 μM (dark gray bars). Part of our data reported for human (h) NAT1/2 (Uno et al., 2018) is also illustrated in panel (C).

sulfamethazine was acetylated by not only macaque NAT2 but also by NAT1 in consideration of a pattern of relative catalytic activities (Uno et al., 2018). These results indicate similarities and differences of substrate selectivity of NAT enzymes among the species tested.

Pig liver cytosolic fractions showed high acetylation levels of sulfamethazine, although pig NAT1 did not efficiently acetylate the reactions (Fig. 5), indicating the possibility that other NAT(s) might be present and play these roles. Analysis of the pig genome found another *NAT* gene (*NAT2*) (Fig. 1) with its expressed sequence tags (ESTs) from bladder found in GenBank (unpublished data); therefore, pig NAT2 mRNA appears to be expressed. However, neither ESTs from liver nor cDNA with a complete reading frame have been reported or deposited to GenBank. Our attempts failed to isolate pig NAT2 cDNA by RT-PCR despite using several different primer pairs in liver, kidney, and small intestine. It would be of great interest to further investigate the presence of pig NAT2.

The differences in acetylation activities observed in marmoset NAT1 and pig NAT1 compared with human NATs might be accounted for by amino acid changes in regions important for NAT function. The residues N95, F97, D99, N103, and A104 in pig NAT1, and A214 in marmoset NAT1 and pig NAT1 are located in regions important for substrate binding (residues 93–106 and 212–222) (Zhang et al., 2006). Of these, residues 103 and 214, among others, form hydrogen bonds, and residue 214 is involved in van der Waals interactions with the substrate CoA (Wu et al., 2007). The residue I131 in marmoset NAT1 is

located in the flexible loop important for substrate specificity (residues 122–131) (Zhang et al., 2006). Pig NAT1 contained a different residue at position 185 from that in human NAT2, which itself shows reduced activity as a result of mutation at residue 185 (Summerscales and Josephy, 2004) (Fig. 2). E276 of marmoset NAT1 and pig NAT1 and K277 of pig NAT1 were different from the residues in human NATs and were located in the *C*-terminal region, which is essential for the enzyme activity and substrate specificity of NAT enzymes (Mushtaq et al., 2002). The *C*-terminal region of human NAT enzymes extends into the interior of the folded enzyme close to the buried catalytic triad and restricts its accessibility (Wu et al., 2007). Amino acid substitutions located in the *C*-terminal region might influence active site access and the substrate specificity of the enzyme.

Several amino acid changes in pig and marmoset NAT1 were found at the same locations as mutated residues present in functional polymorphisms of human NATs, including D167 in marmoset NAT1 and I149 and A214 in marmoset NAT1 and pig NAT1 (Walraven et al., 2008a; Walraven et al., 2008b). In humans, genetic variants are responsible for inter-individual variability of NAT activities toward such substrates as isoniazid, hydralazine, and sulfamethazine, which are acetylated by NAT2 (Sim et al., 2014). Similarly, for marmosets and pigs, genetic variants have been found in drug-metabolizing enzyme genes such as cytochromes P450 (Puccinelli et al., 2011; Uehara et al., 2016a), although information on such genetic variants is currently limited. Investigation of genetic variants might help us to understand the potential inter-animal variability of NAT activities in marmosets and pigs.

In conclusion, marmoset NAT1 and pig NAT1 were identified in this study and showed high sequence identities to human NAT1. These marmoset and pig NAT mRNAs were expressed in various tissues, with the most abundant expression in small intestine. Marmoset NAT1 and pig NAT1 acetylated typical human NAT substrates, including *p*-aminobenzoic acid, 2-aminofluorene, sulfamethazine, and isoniazid, indicating that these NATs are functional enzymes, although substrate specificity differed somewhat from human NAT2. Therefore, marmoset NAT1 and pig NAT1 have similarities and differences in molecular and enzymatic characteristics compared with human NAT1.

Acknowledgments

The authors thank Drs. Erika Sasaki, Takashi Inoue, Takanori Serizawa, Yutaro Noda, and Makiko Shimizu for their assistance. We are also grateful to David Smallbones for copyediting a draft of this article.

Authorship Contributions

Participated in research design: Uno, Uehara, Yamazaki.

Conducted experiments: Uno, Uehara, Banju, Murayama.

Contributed new reagents or analytic tools: Uno, Uehara, Ijiri, Kawaguchi.

Performed data analysis: Uno, Uehara, Asano, Shiraishi, Yamazaki.

Wrote or contributed to the writing of the manuscript: Uno, Uehara, Yamazaki.

References

Boukouvala S and Fakis G (2005) Arylamine N-acetyltransferases: what we learn from genes and genomes. *Drug Metab Rev* **37**:511–564.

Hein DW (2009) *N*-acetyltransferase SNPs: emerging concepts serve as a paradigm for understanding complexities of personalized medicine. *Expert Opin Drug Metab Toxicol* **5**:353–366.

Hickman D, Pope J, Patil SD, Fakis G, Smelt V, Stanley LA, Payton M, Unadkat JD, and Sim E (1998) Expression of arylamine *N*-acetyltransferase in human intestine. *Gut* **42**:402–409.

Husain A, Zhang X, Doll MA, States JC, Barker DF, and Hein DW (2007a) Functional analysis of the human *N-acetyltransferase 1* major promoter: quantitation of tissue expression and identification of critical sequence elements. *Drug Metab Dispos* **35**:1649–1656.

Husain A, Zhang X, Doll MA, States JC, Barker DF, and Hein DW (2007b) Identification of *N*-acetyltransferase 2 (*NAT2*) transcription start sites and quantitation of *NAT2*-specific mRNA in human tissues. *Drug Metab Dispos* **35**:721–727.

Jennne JW (1965) Partial purification and properties of the isoniazid transacetylase in human liver. Its relationship to the acetylation of p-aminosalicylic acid. *J Clin Invest* **44**:1992–2002.

Mushtaq A, Payton M, and Sim E (2002) The COOH terminus of arylamine *N*-acetyltransferase from *Salmonella typhimurium* controls enzymic activity. *J Biol Chem* **277**:12175–12181.

Payton M, Mushtaq A, Yu TW, Wu LJ, Sinclair J, and Sim E (2001) Eubacterial arylamine *N*-acetyltransferases - identification and comparison of 18 members of the protein family with conserved active site cysteine, histidine and aspartate residues. *Microbiology (Reading)* **147**:1137–1147.

Puccinelli E, Gervasi PG, and Longo V (2011) Xenobiotic metabolizing cytochrome P450 in pig, a promising animal model. *Curr Drug Metab* **12**:507–525.

Sim E, Abuhammad A, and Ryan A (2014) Arylamine *N*-acetyltransferases: from drug metabolism and pharmacogenetics to drug discovery. *Br J Pharmacol* **171**:2705–2725.

Sim E, Walters K, and Boukouvala S (2008) Arylamine *N*-acetyltransferases: from structure to function. *Drug Metab Rev* **40**:479–510.

Summerscales JE and Josephy PD (2004) Human acetyl CoA:arylamine *N*-acetyltransferase variants generated by random mutagenesis. *Mol Pharmacol* **65**:220–226.

Uehara S, Uno Y, Inoue T, Kawano M, Shimizu M, Toda A, Utoh M, Sasaki E, and Yamazaki H (2016a) Individual differences in metabolic clearance of *S*-warfarin efficiently mediated by polymorphic marmoset cytochrome P450 2C19 in livers. *Drug Metab Dispos* **44**:911–915.

Uehara S, Uno Y, Inoue T, Sasaki E, and Yamazaki H (2016b) Molecular cloning, tissue distribution, and functional characterization of marmoset cytochrome P450 1A1, 1A2, and 1B1. *Drug Metab Dispos* **44**:8–15.

Uehara S, Uno Y, Okamoto E, Inoue T, Sasaki E, and Yamazaki H (2017) Molecular cloning and characterization of marmoset aldehyde oxidase. *Drug Metab Dispos* **45**:883–886.

Uehara S, Uno Y, and Yamazaki H (2020) Molecular cloning, sequence analysis, and tissue distribution of marmoset monoamine oxidases A and B. *Drug Metab Pharmacokinet* **35**:479–482.

Uno Y, Fujino H, Kito G, Kamataki T, and Nagata R (2006) CYP2C76, a novel cytochrome P450 in cynomolgus monkey, is a major CYP2C in liver, metabolizing tolbutamide and testosterone. *Mol Pharmacol* **70**:477–486.

Uno Y, Murayama N, and Yamazaki H (2018) Molecular and functional characterization of *N*-acetyltransferases NAT1 and NAT2 in cynomolgus macaque. *Chem Res Toxicol* **31**:1269–1276.

Uno Y, Murayama N, and Yamazaki H (2020) Genetic variants of *N*-acetyltransferases 1 and 2 (NAT1 and NAT2) in cynomolgus and rhesus macaques. *Biochem Pharmacol* **177**:113996.

Uno Y, Uehara S, and Yamazaki H (2016) Utility of non-human primates in drug development: Comparison of non-human primate and human drug-metabolizing cytochrome P450 enzymes. *Biochem Pharmacol* **121**:1–7.

Walraven JM, Trent JO, and Hein DW (2008a) Structure-function analyses of single nucleotide polymorphisms in human *N*-acetyltransferase 1. *Drug Metab Rev* **40**:169–184.

Walraven JM, Zang Y, Trent JO, and Hein DW (2008b) Structure/function evaluations of single nucleotide polymorphisms in human *N*-acetyltransferase 2. *Curr Drug Metab* **9**:471–486.

Wu H, Dombrovsky L, Tempel W, Martin F, Loppnau P, Goodfellow GH, Grant DM, and Plotnikov AN (2007) Structural basis of substrate-binding specificity of human arylamine *N*-acetyltransferases. *J Biol Chem* **282**:30189–30197.

Zhang N, Liu L, Liu F, Wagner CR, Hanna PE, and Walters KJ (2006) NMR-based model reveals the structural determinants of mammalian arylamine *N*-acetyltransferase substrate specificity. *J Mol Biol* **363**:188–200.

Zhou X, Ma Z, Dong D, and Wu B (2013) Arylamine *N*-acetyltransferases: a structural perspective. *Br J Pharmacol* **169**:748–760.

Address correspondence to: Dr. Yasuhiro Uno, Joint Faculty of Veterinary Medicine, Kagoshima University, 1-21-24 Korimoto, Kagoshima-city, Kagoshima 890-0065, Japan. E-mail: unoxx001@vet.kagoshima-u.ac.jp; or Dr. Hiroshi Yamazaki, Laboratory of Drug Metabolism and Pharmacokinetics, Showa Pharmaceutical University, 3-3165 Higashi-Tamagawa Gakuen, Machida, Tokyo 194-8543, Japan. E-mail: hyamazak@ac.shoyaku.ac.jp